Nuclear Instruments and Methods in Physics Research A 333 (1993) 391–398
North-Holland

NUCLEAR
INSTRUMENTS
& METHODS
IN PHYSICS
RESEARCH
Section A

Some studies of the applications of CsI photocathodes in gaseous detectors

G. Charpak [a], I. Gaudean [a], Y. Giomataris [b], V. Peskov [c], D. Scigocki [a], F. Sauli [a] and D. Stuart [d]

[a] *PPE Division, CERN, Geneva, Switzerland*
[b] *Lausanne University, Switzerland*
[c] *Fermi National Accelerator Laboratory (FNAL), BT, USA*
[d] *University of California, Davis, CA, USA*

Received 4 March 1993

Cesium-iodide photocathodes have been investigated in combination with gaseous detectors. The quantum efficiency of a semi-transparent CsI photocathode has been measured in the UV range and found to be 10% at 140 nm. We report experimental results obtained with such photocathodes coupled to BaF_2 and $KMgF_3$ scintillators and read out by parallel-plate gaseous detectors.

1. Introduction

Reflective CsI photocathodes have been shown to work with amplifying gaseous detectors [1,2]. A major step in their potential importance comes from two observations [3]: i) The quantum efficiency of reflective CsI photocathodes, when handled under clean conditions, is significantly higher than the one observed in previous experiments. ii) Adsorbed vapours of tetrakis(dimethylamine)ethylene (TMAE) enhance the quantum efficiency and, in addition, protect the CsI in the case of contact with air. This opens up a new way to read out light from scintillators, and Cherenkov light in the case of RICH counters and hadron blind detectors, and has triggered active research [4–9].

We have performed several measurements connected mainly with three applications:
- Readout of $KMgF_3$ crystals for a pre-preshower detector [10].
- Readout of BaF_2 crystals for a preshower counter [10] and for a calorimeter [11].

We have limited our efforts to the combination of CsI photocathodes with parallel-plate gaseous detectors because of their good time resolution (< 1 ns) [12,13].

We have studied the merits of reflective and semi-transparent photocathodes, and have completed ageing measurements in view of the possible applications of the detectors to high-luminosity colliders.

2. Preshower counter

Recently, it was reported that $KMgF_3$ emits at even shorter wavelengths than BaF_2 (between 140 and 220 nm with a decay time of about 2 ns) [14]. Such a spectrum overlaps very well with the quantum efficiency of some solid photocathodes (see for example ref. [15]). Our latest tests show however that the best photocathode for the readout of the $KMgF_3$ scintillation light is still CsI. A thin $KMgF_3$ crystal coupled to a parallel-plate avalanche chamber (PPAC) with a CsI photocathode can be used as a first-step detector in front of a calorimeter in order to distinguish electrons from gammas. A thin crystal of the $KMgF_3$ would detect energy deposited by charged particles, but be nearly transparent to gammas, allowing differentiation between showers created by gammas and electrons. Its advantages are the radiation hardness, and the sub-nanosecond time resolution provided by the $KMgF_3$–PPAC combination.

We have investigated the response of 3 mm and 10 mm thick $KMgF_3$ crystals using a photomultiplier and a PPAC with a CsI photocathode.

2.1. Photomultiplier measurements

We used electrons from a ^{90}Sr source to compare the response of the $KMgF_3$ crystal and a $20 \times 20 \times 50$ mm^3 BaF_2 crystal. The source contains a ^{90}Y compo-

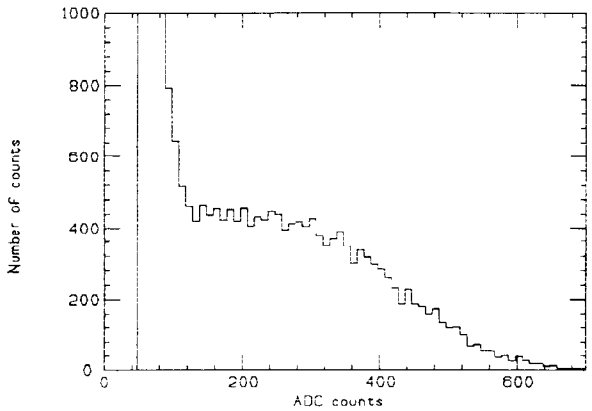

Fig. 1. Typical β spectrum from ^{90}Sr with a maximum energy of 2.2 MeV β obtained with a photomultiplier and a $KMgF_3$ crystal.

nent which emits electrons with a maximum energy of 2.2 MeV. The scintillation light of the crystals is detected by a Hammamatsu R1460 photomultiplier which is sensitive from 110 to 300 nm. A typical spectrum pulse height is shown in fig. 1. By comparing the light output at the 2.2 MeV edge from BaF_2 and from $KMgF_3$, we deduce that the light output of $KMgF_3$ is about 30% of that of the fast component of BaF_2. This corresponds to roughly 100 photoelectrons per MeV, with good optical contact between the crystal and the window.

2.2. PPAC measurement

2.2.1. Setup

A small PPAC was built as shown in fig. 2. It consists of a $KMgF_3$ scintillator, an anode mesh, and a copper pad cathode 4 mm away. A CsI layer 200 or 500 nm thick was deposited either on the copper pads or directly on the $KMgF_3$ scintillator, covered by a 20 nm layer of W. This is only a slight modification of the setup used in ref. [11]. In the present work we used a mixture of He with a few percent of C_2H_6 or CH_4 at atmospheric pressure. The gas and electronic gains were calibrated with a ^{55}Fe source. This allowed us to measure directly the primary charge (number of photoelectrons) of the signals from the crystal.

2.2.2. Results

Although many studies were made on reflective CsI photocathodes, no systematic study was carried out to compare such a photocathode with a semi-transparent one. On the other hand, for some applications the semi-transparent photocathode may have advantages. For example, in the case of crystal readout it can be expected that more scintillation light will penetrate a semi-transparent CsI photocathode because the difference in refractive index is smaller between the crystal and the CsI than CsI and gas. To study this we did some measurements with the semi-transparent CsI photocathode. Some results of the quantum efficiency measurements are presented in fig. 3. It can be concluded from this figure that the quantum efficiency of the reflective CsI photocathode is considerably higher than that of the semi-transparent one.

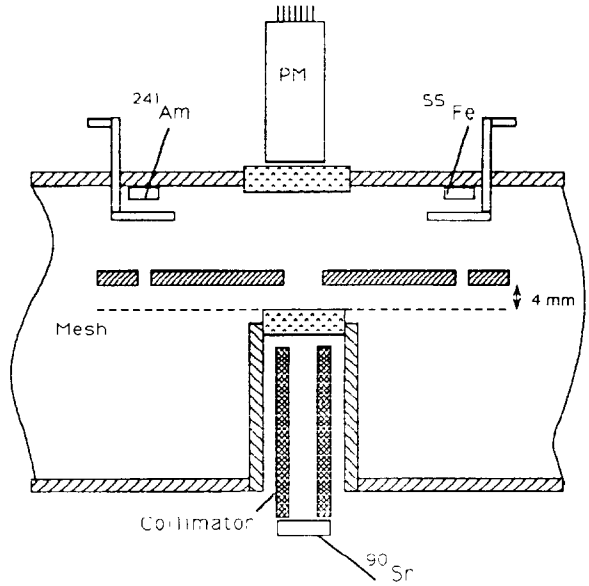

Fig. 2. Diagram of a PPAC with a CsI photocathode used to measure $KMgF_3$ scintillation.

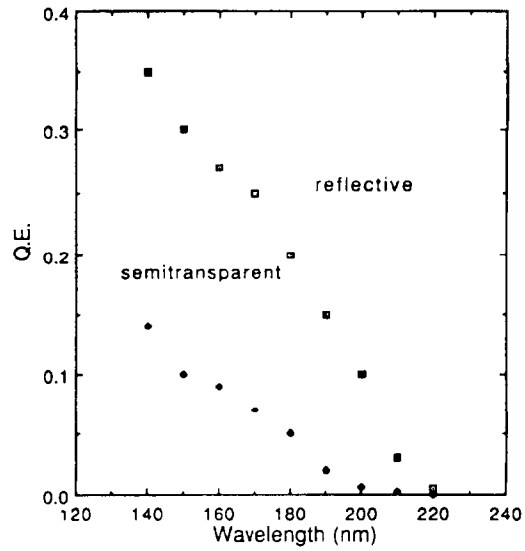

Fig. 3. Quantum efficiency of a reflective and a semi-transparent CsI photocathode 500 mm thick.

The spectrum obtained with ^{90}Sr from the PPAC with the reflective CsI photocathode and a 3 mm thick crystal is shown in fig. 4. Note that it does not exhibit the shape shown in fig. 1, but is rather exponentially peaked towards zero. We estimate that the 2.2 MeV β-edge corresponds to roughly 40 photoelectrons of primary charge. In the case of a 10 mm crystal the result was 20 photoelectrons. The difference may be partly due to crystal quality. When comparing with a photomultiplier (100 e^- per MeV) we have to take into account the absorption in the grid and the internal reflection losses due to the absence of optical contact.

Assuming an energy loss of 3 MeV/cm for a minimum ionizing particle (MIP) in $KMgF_3$, we expect at least 20 photoelectrons of primary charge from the passage of a MIP through a 3 mm thick crystal. This can be easily detected using a PPAC with a CsI photocathode. The radiation length of $KMgF_3$ is 7.5 cm, which should give an e–γ selection of about 7%.

Results obtained with the semi-transparent CsI photocathode were much more modest. Although we expected better scintillation light collection, only a few photoelectrons were created from the photocathode with the deposited energy of 2.2 MeV. We conclude from these measurements that a reflective CsI photocathode is superior to a semi-transparent one. For this reason we only used reflective photocathodes in the latest experiments.

3. BaF_2 preshower counter

A preshower counter in front of a calorimeter is needed for high-precision position measurements of the showers and to increase the e/π rejection capability. Such a device may be necessary not only for the BaF_2 calorimeter, described later in this paper, but also for many of the detector candidates for the calorimetry to be used in experiments at the future high-luminosity colliders. A preshower counter made from 2.5 radiation lengths of BaF_2 crystal with a PPAC readout and a CsI photocathode was suggested in ref. [11]. Minimum ionizing particles will deposit 32 MeV in the detector; an electromagnetic shower will deposit a few hundred MeV. For the typical photocathode efficiency we expect to have a few photoelectrons per MeV deposited in the BaF_2. In this case the gain needed in the PPAC is about 10^3–10^4. The position of the shower, or of the MIPs, can be measured on the pads by the centre-of-gravity method, and the difference in the energy deposited will make it possible to measure the e/π separation in the preshower counter.

The main advantages of the BaF_2 preshower counter are: high radiation resistance (up to Mrad), good time resolution ($\sim$ 1 ns), and the possibility of measuring the deposited energy. In order to check these advantages and especially measure the space resolution we made and tested in the laboratory a small prototype of the BaF_2 preshower counter.

3.1. Construction

The installation used to test the BaF_2 preshower counter is shown in fig. 5. The detector used a BaF_2 crystal of 12 cm diameter and 1 cm thickness as the window and the scintillator. The active size of the cathode plane and of the wire plane is 200×200 mm^2, with 1600 pads. At high gain and with a high flux of particles the PPAC may suffer from sparks [16]. The problem has been completely eliminated in this work

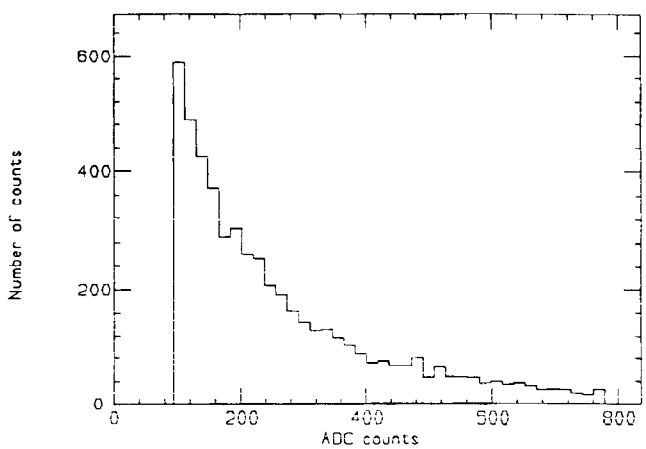

Fig. 4. Charge spectrum from a PPAC with $KMgF_3$ irradiated by a ^{90}Sr source. The 5.9 keV from ^{55}Fe, absorbed in the drift space, was used to calibrate the gain in the gap.

by loading each anode wire with a 10 MΩ resistor. The resistor limits the current and makes the transition of a streamer into a spark almost impossible.

A high voltage is applied on the anode wires, and the signal is read out on each pad with a charge amplifier as described above. The PPAC worked with a gas mixture composed of He + 1% CH_4 + ~ 10^{-2} Torr of ethyl ferrocene (EF) at atmospheric pressure.

The reflective photocathode is deposited on the pads by vacuum evaporation. Immediately after the 500 nm thick CsI photocathode was deposited, the cathode plane was transferred to a box where it was pumped before being put into contact with the EF vapour. The photocathode was in contact with air for less than 2 min., and after a few hours of gas flushing with EF vapour + argon, an adsorbed layer of EF had formed and protected the photocathode from the reaction with air. Then the photocathode was mounted in the detector in air.

The scintillation of the BaF_2 crystal was produced by a pulsed (~ 10 ns) X-ray source with the maximum energy of photons ~ 60 keV. This source could deposit an equivalent energy of up to 100 GeV per pulse. If necessary, this energy can be reduced by a set of lead attenuators. In most measurements a lead collimator (a hole of 500 μm) was used to simulate a single-particle crossing.

In some tests a pulsed (15 ns) vacuum ultraviolet (VUV) source was also used to extract electrons from the CsI photocathode.

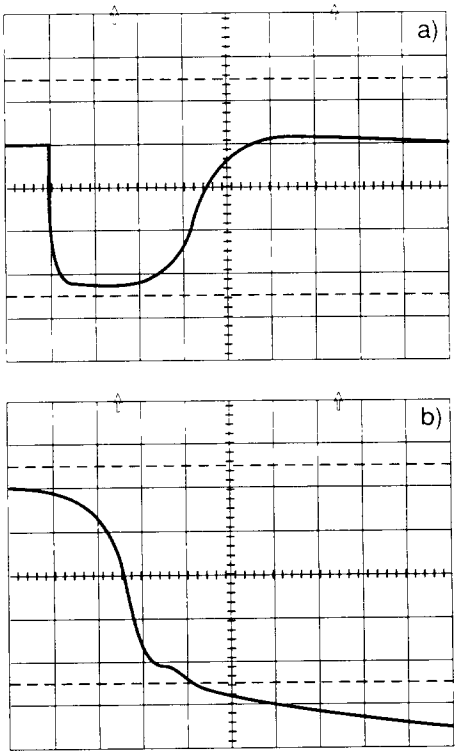

Fig. 6. PPAC signal from the preshower detector at 2.6 kV. (a) The horizontal scale is 5 μs per division and the vertical scale is 50 mV per division. (b) The horizontal scale is 50 ns per division and the vertical scale is 100 mV per division

4. Results

Fig. 6a shows the signal obtained from the collimated pulsed X-ray generator at an applied voltage of 2.6 kV. The electron part of the signal is shown better in fig. 6b. Our measurements were made starting from the ionization chamber mode (gain 1) and up to gain 10^6. The typical dependence of the gain on the voltage is shown in fig. 7. The detector can work in a stable fashion at a high gain of 10^5. Fig. 8a shows the profile of the collimated pulsed X-ray generator signal on a line of pads. Each bin represents one pad (10 mm). The vertical axis is the collected charge on the corresponding ADC. Fig. 8b is a similar measurement in the same geometry, but with a pulsed UV source which produces a spot of light of a few mm diameter on one pad. The spread due to the scintillation light in the crystal is clearly shown by comparing the two figures as well as is the negligible contribution due to the avalanche size in the PPAC. It can be seen that the position of the avalanches can be defined by a centre-of-gravity method. The uniformity of the signal between the pads was measured to be better than 15%.

The energy resolution of the detector at a gas gain of 10^5 is shown in fig. 9. In this test about 10 photoelectrons were injected by the attenuated light beam from the VUV pulsed lamp. An energy resolution of 70% FWHM was achieved, which confirms the results

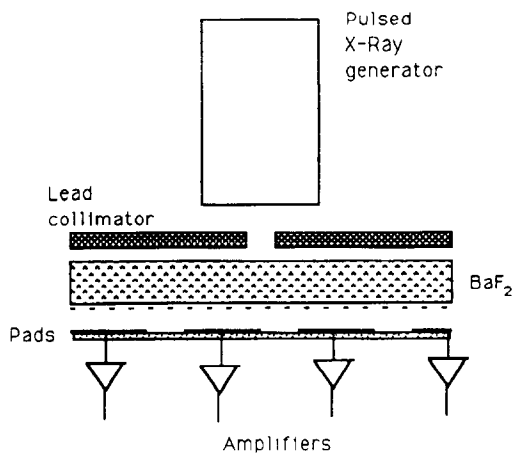

Fig. 5. Experimental setup for the study of the BaF_2 preshower prototype.

obtained in ref. [11]. Although these preliminary results are encouraging, the prototype has to be tested in a beam to measure precisely the position resolution for electrons and gamma photons, as well as the electron–pion rejection capability.

5. Test of a prototype of a BaF_2 calorimeter module

A BaF_2 calorimeter is being discussed as a possible candidate for the LHC and SSC experiments (see for example ref. [17]). A possible layout of a BaF_2 calorimeter for the SSC and LHC experiments is described in refs. [17,18]. It consists of an array of BaF_2 crystals covering the acceptance $|\eta| < 3.8$. Photodiodes were proposed for the readout of the fast component (~ 1 ns) of the scintillation light with $\lambda < 220$ nm.

We developed another approach, based on the PPAC with a solid photocathode. The main advantage of this type of readout compared to that of photodiodes is that the PPAC itself is very cheap and allows gas gain. A first prototype of this type of readout was tested by the authors of ref. [18]. The energy resolution was measured as $3\%/\sqrt{E}$ at gain 1 [19] and 7% at gain 10^5 [11]. In this section we present some results of tests of one calorimeter module with PPAC readout of the fast BaF_2 scintillation light.

5.1. Experimental setup

The prototype of the BaF_2 calorimeter module is presented in fig. 10. It consists of a BaF_2 crystal 200 mm long and 55 mm in diameter directly coupled to the PPAC. The PPAC is built from the anode mesh and the stainless-steel (ss) cathode plane 70 mm in diameter and 7 mm away. The anode mesh was put at 1 mm distance from the BaF_2 crystal in order to avoid possible charging of the crystal by the colliding electrons. The stainless-steel cathode plane was covered by a 55 nm thick CsI layer with an EF adsorbed film by a procedure similar to the one described above. The pure CsI was first deposited on the cathode by the vacuum evaporation technique and mounted inside the detector in a glove box flushed with argon to limit the contact with air. Then the EF adsorbed layer was formed by continuously flushing the gas mixture containing EF vapour through the gaseous detector.

In this test the gaseous detector was mainly used in ionization chamber mode with a gas mixture composed of He + different concentrations of CH_4 + $\sim 10^{-2}$

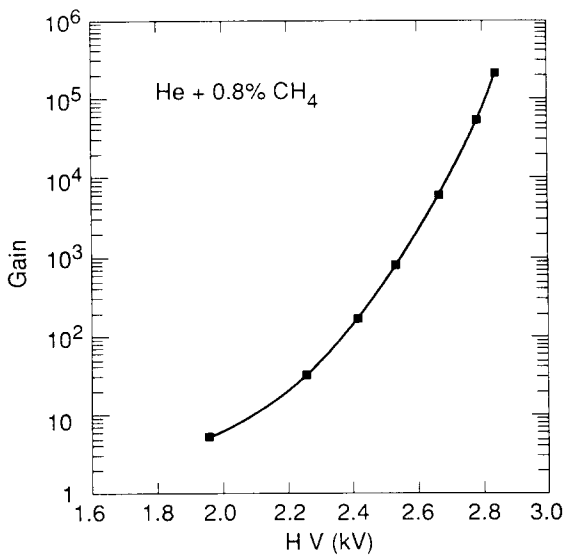

Fig. 7. Gain measurements of the preshower detector with a gas mixture composed of He + 0.8% CH_4 + 10^{-2} Torr of EF vapour.

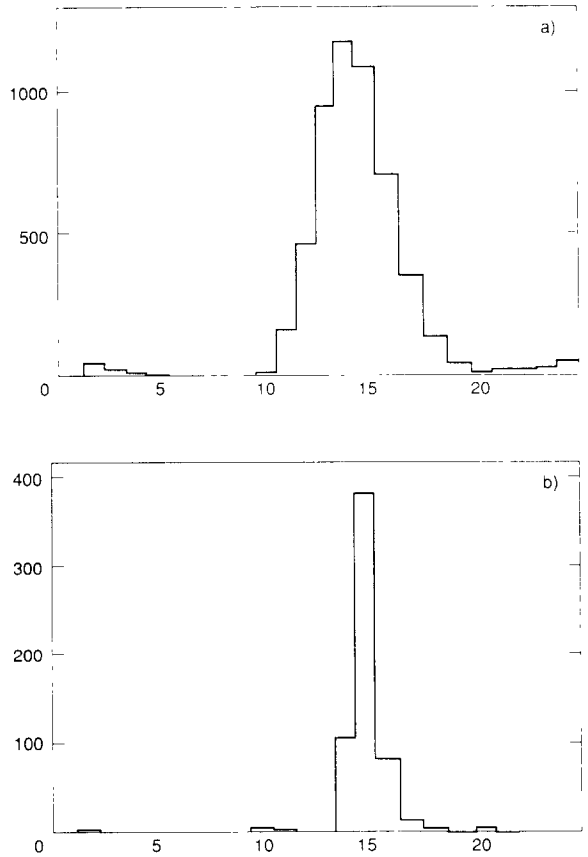

Fig. 8. (a) Profile on the pads for the collimated pulsed X-ray generator. Each line on the horizontal axis represents a pad number and the vertical axis represents the charge collected on the ADC. (b) A similar picture for a pulsed UV lamp signal with the same geometry. The size of the light spot on the pad is a few mm in diameter

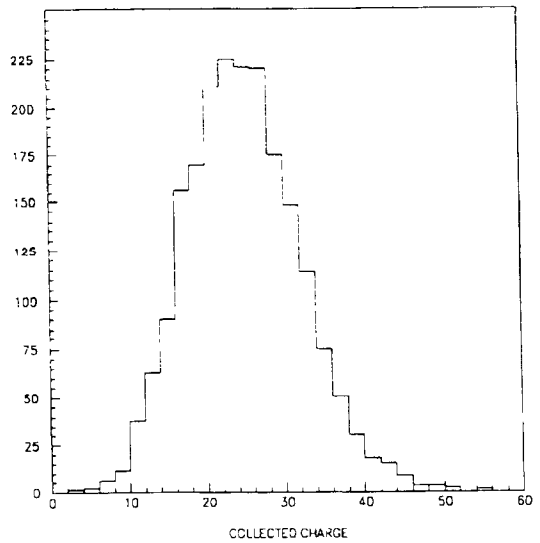

Fig. 9 Pulse distribution obtained from the PPAC irradiated by the VUV source extracting 10 photoelectrons per pulse from the CsI photocathode.

Torr of EF vapour (~ 50% of EF vapour pressure at room temperature).

The ionization source was the pulsed (~ 10 ns) X-ray generator mentioned earlier (see fig. 5). Using a set of lead absorbers we could decrease this energy. The HV was applied on the cathode, and the signal was read out on the grid with a fast charge amplifier (rise time < 10 ns, 360 mV per pC). A photomultiplier was mounted directly (see fig. 10) on the crystal to monitor the deposited energy by measuring the intensity of scintillation light with $\lambda < 220$ nm.

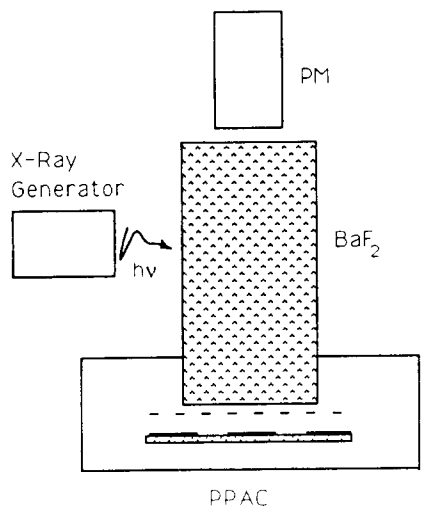

Fig. 10. Experimental setup for the study of the BaF_2 prototype calorimeter cell

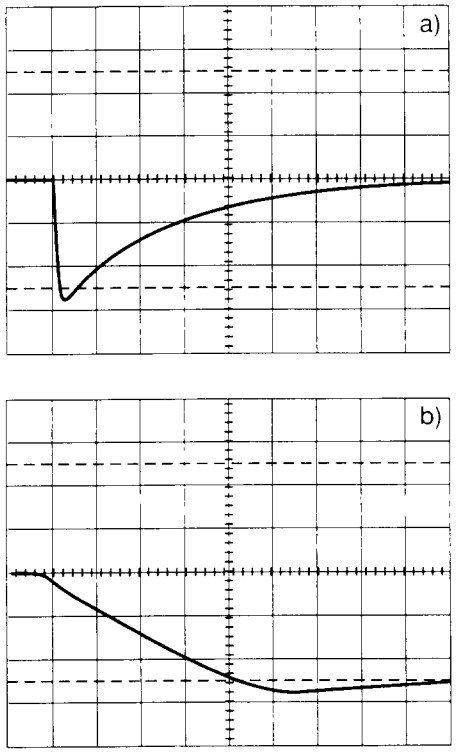

Fig. 11. Ionization chamber signal at 1 kV (a) The horizontal scale is 1 μs per division and the vertical scale is 20 mV per division. (b) The horizontal scale is 50 ns per division and the vertical scale is 20 mV per division.

5.2. Results

A typical ionization chamber signal obtained in the mixture He + 1% CH_4 + EF (10^{-2} Torr) is shown in fig. 11.

The rise-time of the signal is about 200 ns. The drift velocity is about 50 ns/mm for an electric field of 2.5 kV/cm. For pure CH_4 and higher fields, the drift velocity reached about 10 ns/mm.

The signal correlation between the ionization chamber and the photomultiplier is shown in fig. 12. The average maximum signal in the gaseous detector was about 600000 photoelectrons which corresponds to a deposited energy of about 100 GeV. The energy resolution was 0.73% rms.

Analysis of the data, obtained with the lead attenuator, when the deposited energy was decreased by a factor of 2, shows that the energy resolution remains practically unchanged at ~ 0.7 rms., indicating that the constant term is dominating. This qualitatively con-

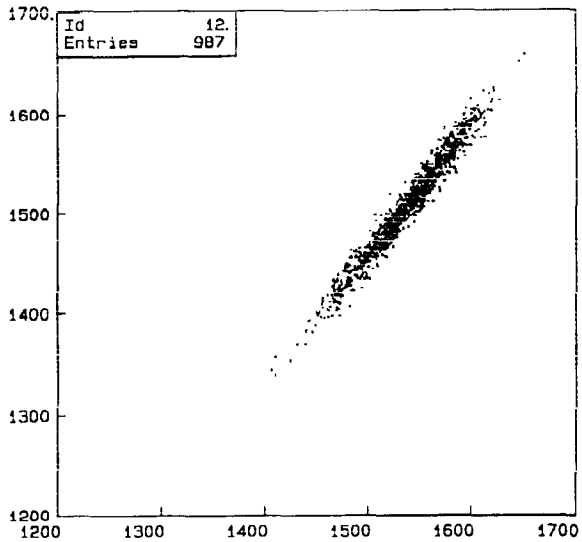

Fig. 12. Correlation between the ionization chamber and the photomultiplier for the pulsed X-ray generator signal.

firms results obtained in ref. [19]: the energy resolution is

$$< 3\%\ E^{-1/2}[\mathrm{GeV}] + 0.5\%.$$

It should be noted that the detector worked for more than three months with high stability using the same photocathode. CsI photocathodes covered with TMAE or EF adsorbed layers were observed earlier to be more resistant to air than pure CsI layers [10,18]. We have verified this phenomenon for EF with our detector. The photocathode was exposed to air for four hours. The signal decreased by only 9%. After flushing with gas for one day full recovery was observed.

As was mentioned in the introduction, one of the advantages of this type of readout is the possibility to work with gas gain. This could be useful for the calorimeter design where the crystal is segmented along the shower axis, as was suggested in ref. [10]. Gas gain could be useful in the parts corresponding to the beginning and the end of the shower, where the deposited energy is relatively low. Our preliminary study shows that although with a gain of about 10, energy resolution is already degraded, this will not noticeably affect the energy resolution of the calorimeter.

6. Ageing properties of the CsI photocathodes

After the observation that the CsI photocathode could be used successfully for the readout of the BaF_2 calorimetry and the preshower counters, the crucial point is the stability and ageing properties of the photocathode.

Concerning these questions there is some controversy in the literature. In some works [3,12,20] it was found that the CsI photocathode irradiated continuously by the VUV light slow one. In the case of the fast component the quantum efficiency drops by a factor of e at a collected charge of about $Q_f \sim 0.5$ nC/cm^2; in the case of the slow component at a charge $Q_{sl} < 5$ mC/cm^2. In one work [21] it was reported that the collected charge for which the slow component degrades by a factor e is approximately $Q_{sl} < 100$ mC/cm^2.

The contradictions in the measured values of Q_{sl} could be explained by the results obtained in ref. [22]. It was first shown in this work that the degradation in the CsI quantum efficiency is reversible in most cases, by keeping the photocathode for some time without VUV radiation or by warming it up to 90°C. This explains why in ref. [21] Q_{sl} was achieved 200 times better than in ref. [3]: in ref. [21] the quantum efficiency of the photocathode was measured one hour later, after the VUV beam was shut down.

Taking into account the observation made in ref. [22] we carried out a study of the stability of the CsI quantum efficiency. The results, described in ref. [22], were confirmed both in vacuum and in a gas atmosphere. At low VUV flux (corresponding to a current ≤ 1 nA) and clean gas conditions (stainless-steel tubes, oxisorb filter) no indication of the degradation of quantum efficiency was observed up to the collected charge ~ 100 mC/cm^2. The same results were obtained at a gas gain of 10–20. These ageing properties are enough for recording the scintillation light from the BaF_2 corresponding to ~ 10 Mrad deposited energy. Nevertheless, the radiation properties of the CsI photocathode itself should be studied.

7. Conclusion

We have investigated the scintillation of a $KMgF_3$ crystal using both a photomultiplier and a photosensitive PPAC with a CsI photocathode. We found that the photomultiplier signal from $KMgF_3$ is 30% of the signal for the BaF_2 fast component. The PPAC sensitivity with BaF_2 was about 20 photoelectrons per MeV deposited energy, which will allow detection of MIPs using a thin crystal. This shows the interest of putting such a counter in front of calorimeters. The advantage over other types of detectors is the time resolution of the order of 1 ns together with the radiation hardness.

In studying the coupling of BaF_2 to the PPAC we have made some progress in the construction of BaF_2 high-granularity preshower detectors and electromagnetic calorimeters with properties matching the re-

quirements of future colliders, i.e. fast timing, radiation hardness, and good granularity and energy resolution.

In addition, the construction techniques for the detector are simple, owing to the resistance to air of the photocathode which works at room temperature and atmospheric pressure, and no window is needed between the scintillator and the gaseous detector. Therefore the price of such a readout is negligible compared to that using other classical techniques, such as photodiodes. For application to high-luminosity machines, the ageing properties of the photocathodes are of prime importance. Our latest results indicate that CsI is not modified by irradiations in the range 100 mC/cm^2. As a final demonstration, a prototype of a large enough size has to be built and tested in a beam environment.

Acknowledgements

This work was performed in the frame of the LAA project and we thank Prof. A. Zichichi for his support and discussions, and R. Bouclier, I. Croty and G. Million for their technical support.

References

[1] G. Charpak et al., preprint CERN EP/89-66 (1989).
[2] V. Daugendorf et al., Nucl. Instr. and Meth. A289 (1990) 322.
[3] J. Seguinot et al., Nucl. Instr. and Meth. A297 (1990) 133.
[4] B. Hoeneisen et al., Nucl. Instr. and Meth. A302 (1991) 447.
[5] B. Guerard et al., Nucl. Instr. and Meth. A310 (1991) 116.
[6] D. Imrie et al., Nucl. Instr. and Meth. A310 (1991) 122.
[7] Y. Giomataris and G. Charpak, Nucl. Instr. and Meth. A310 (1991) 589.
[8] M. Staric et al., Nucl. Instr. and Meth. A307 (1991) 145.
[9] R. Arnold et al., University Louis Pasteur preprint CRN/HE-91-06 (1991).
[10] G. Charpak et al., Proc. Large Hadron Collider Workshop, Aachen, 1990, eds. G. Jarlskog and D Rein, CERN 90-10, EFCA 90-133 (1990), vol. 3, p 384.
[11] G. Charpak et al., Proc. 9th INFN Workshop on Perspectives for New Detectors in Future Supercolliders, Italy, 1989, eds. L. Cifarelli, R. Wigmans and T. Ypsilantis (World Scientific, Singapore, 1991), p. 43;
G. Charpak et al., preprint CERN-EP/90-41 (1990).
[12] G Charpak et al., Nucl. Instr. and Meth. A307 (1991) 63.
[13] V. Daugendorf et al., Nucl. Instr. and Meth. A308 (1991) 519.
[14] J.L. Janson et al., Solide State Commun 67 (1988) 183.
[15] D Imrie et al. (paper in preparation).
[16] P. Fonte et al., Nucl Instr. and Meth. A305 (1991) 91.
[17] S.C. Ting (spokesman), Expression of interest to the SSC Laboratory by the L Collaboration, May 1990.
[18] R. Zhu, Proc. Large Hadron Collider Workshop, Aachen, 1990, eds. G. Jarlskog and D. Rein, CERN 90-10, EFCA 90-133 (1990), vol 3, p. 411.
[19] Y. Giomataris et al (unpublished data).
[20] S. Kwan et al., preprint Fermilab-Pub 91/98 (1991).
[21] G. Charpak et al., Nucl. Instr and Meth. A310 (1991) 128.
[22] D. Anderson et al., Fermilab Tech. Memo TM-1753 (1991).